532 (1991); N. Tanaka and T. Taniguchi, unpublished results.
10. H. Harada *et al.*, *Science* **259**, 971 (1993).
11. A. Abdollahi, K. A. Lord, B. Hoffman-Liebermann, D. A. Liebermann, *Cell Growth Differ.* **2**, 401 (1991).
12. K. Huebner *et al.*, *Science* **230**, 1282 (1985); A. W. Nienhuis *et al.*, *Cell* **42**, 421 (1985); M. M. Le Beau *et al.*, *Science* **231**, 984 (1986); M. M. Le Beau *et al.*, *Proc. Natl. Acad. Sci. U.S.A.* **84**, 5913 (1987); G. R. Sutherland *et al.*, *Blood* **71**, 1150 (1988); J. A. Warrington *et al.*, *Genomics* **13**, 803 (1992).
13. H. Sartor, F. Ehlert, K.-H. Grzeschik, R. Muller, S. Adolph, *Genomics* **13**, 911 (1992); T. Meeker, W. L. Kuo, M. Pallavicini, C. Sever, C. Willman, unpublished results.
14. DNA was prepared from normal peripheral blood lymphocytes that had been suspended in 0.5% low-melting agarose at a concentration of 5×10^5 cells per agar plug [J. Sambrook, E. F. Fritsch, T. Maniatis, *Molecular Cloning: A Laboratory Manual* (Cold Spring Harbor Laboratory, Cold Spring Harbor, NY, ed. 2, 1989)]. Samples were digested for 16 hours with 10 to 20 units of the indicated enzymes (Fig. 1B) per plug, and the resulting fragments subjected to PFGE on a CHEF-DR™II system to resolve bands from 200 to 2000 kb. After transfer to nitrocellulose, the separated fragments were hybridized with cDNA probes for *IL-4, IL-5, IRF-1, CDC25C, IL-3,* and *GM-CSF* that had been labeled by the random primer method.
15. M. Maruyama, T. Fujita, T. Taniguchi, *Nucleic Acids Res.* **17**, 3292 (1989).
16. R. G. DiScipio *et al.*, *Proc. Natl. Acad. Sci. U.S.A.* **81**, 7298 (1984); C. Abbot *et al.*, *Genomics* **4**, 606 (1989).
17. Striking heterogeneity was observed in the deletion of *IL-4, IL-5, CDC25C,* and *GM-CSF* among different samples. Although Samples 3 and 8 were initially shown to have distal breakpoints at 5q35 and 5q33, respectively, deletion analysis indicated that the distal breakpoint in each case was between *IRF-1* and *CDC25C* (Table 1). Analysis of patients with the smallest deletions (Sample 10, *IRF-1* only; Sample 11, *IRF-1* and *CDC25C*; Sample 13, *IRF-1* only) revealed that *IRF-1* was the only consistently deleted gene.
18. Genomic DNA (1 μg) from the leukemic sample (Table 1, Sample 10) and normal DNA were digested in a 100-μl reaction volume with Hind III (10 units) at 37°C for 3 hours. Digested DNA was diluted to 2 μg/ml in ligase buffer [50 mM tris-HCl (pH 7.6), 10 mM $MgCl_2$, 1 mM ATP, 1 mM dithiothreitol] and incubated with 2.8 units of T4 DNA ligase at 14°C for 20 hours. After ligation, the DNA was resuspended in distilled H_2O (30 μl), and nicks were introduced by heating at 95°C for 10 min. The regions encompassing *IRF-1* exon 1 and intron 1 were amplified by PCR (DNA thermal cycler, Perkin-Elmer Cetus) with the primers indicated in Fig. 2C. Primer 1 was 5′-CGCGCACGCAGATCTGCGAAACCTG-3′ (the Bgl II site is underlined), and primer 2 was 5′-TTCCAACCAAATCCCGGGGCTCATC-3′. The reaction was carried out (95°C for 30 sec, 60°C for 1 min, 70°C for 2 min, 40 cycles) in 50-μl volumes with 1 μM $MgCl_2$, 0.01% gelatin, and 1.25 units Taq I DNA polymerase (Perkin-Elmer Cetus). The PCR products were checked by agarose gel electrophoresis, and the appropriate bands (a 1.1-kb Hind III fragment from normal DNA and a 0.4-kb Hind III fragment from leukemic DNA) were cloned into the Bluescript plasmid. The sequence from primer 2 to the 3′ Hind III site (Fig. 2C) in six independently isolated clones was identical in normal and leukemic DNA; the leukemic DNA sequence diverged from the normal sequence beginning ten nucleotides 5′ to primer 1 and was thereafter replaced with an unknown sequence. The PCR fragment obtained from normal DNA hybridized to the expected *IRF-1* restriction fragments, whereas the 0.4-kb fragment derived from leukemic DNA hybridized to novel bands detected in Southern blots (Fig. 2B).
19. K. W. Kinzler *et al.*, *Science* **251**, 1366 (1991).
20. H. Harada, C. Sever, C. Willman, T. Taniguchi, unpublished results.
21. Probes detecting *IRF-1* or 5q22 sequences were differentially labeled to allow single (*IRF-1*) or dual (*IRF-1* and 5q22) color visualization of hybridized domains in interphase cells from MDS and leukemic samples (*7*). Single- and dual-color hybridizations were performed by a modification of the procedures described in Kuo *et al.* (*7*). (The authors will supply a detailed procedure upon request.) Fluorescence microscopy with appropriate filters was accomplished as described in Pinkel *et al.* (*7*). In single-color studies, all cells in the microscopic field were scored as having two, one, or no *IRF-1* domains (Table 1). In dual-color studies, *IRF-1* domains were scored in cells showing at least one 5q22 hybridization domain. Blast populations definitively lacking one *IRF-1* hybridization domain but retaining one 5q22 hybridization domain were identified in 4 of 16 residual cells that could be analyzed in Sample 10.
22. D. A. Haber *et al.*, *Cell* **61**, 1257 (1990); G. Xu *et al.*, *ibid.* **62**, 599 (1990); J. Groden *et al.*, *ibid.* **66**, 589 (1991); C. J. Marshall, *ibid.* **64**, 313 (1991); K. W. Kinzler *et al.*, *Science* **253**, 661 (1991); Y. Li *et al.*, *Cell* **69**, 275 (1992).
23. We thank T. Montoya and B. Griffith for excellent technical assistance; J. Gray, C. Sherr, Y. Nakamura, M. Kitagawa, and M. Lamphier for helpful discussions and comments; D. Boldt, D. Head, A. Sandberg, R. Morgan, T. McConnell, and S. Kerman for submission of karyotypes and morphologic slide review; and S. Curtin for expert manuscript preparation. This work was supported by Department of Health and Human Services grants CA-32734 and CA-32102 (to the Southwest Oncology Group Leukemia Biology Program), DK-43042 (to C.W.), CA-44047 (to M.P.), and CA-33572 (to M.S.); and by a grant-in-aid for Special Projects Research, Cancer Bioscience, from the Ministry of Education, Science, and Culture of Japan. C.S. was also supported by an American Cancer Society Clinical Oncology Fellowship Award.

15 October 1992; accepted 16 December 1992

Anti-Oncogenic and Oncogenic Potentials of Interferon Regulatory Factors–1 and –2

Hisashi Harada,* Motoo Kitagawa,* Nobuyuki Tanaka, Hitomi Yamamoto, Kenji Harada, Masahiko Ishihara, Tadatsugu Taniguchi

Interferon regulatory factor–1 (IRF-1), a transcriptional activator, and IRF-2, its antagonistic repressor, have been identified as regulators of type I interferon and interferon-inducible genes. The *IRF-1* gene is itself interferon-inducible and hence may be one of the target genes critical for interferon action. When the *IRF-2* gene was overexpressed in NIH 3T3 cells, the cells became transformed and displayed enhanced tumorigenicity in nude mice. This transformed phenotype was reversed by concomitant overexpression of the *IRF-1* gene. Thus, restrained cell growth depends on a balance between these two mutually antagonistic transcription factors.

Interferons (IFNs) are a family of cytokines that exhibit antiproliferative activity on many normal and transformed cells and can block growth factor–stimulated cell cycle transitions (*1*). IFNs are induced by growth factors, which suggests that they participate in a feedback mechanism that regulates cell growth (*1*). In previous studies, we identified two DNA binding factors that regulate *IFN* gene expression, IRF-1 and IRF-2 (*2–5*). These factors are structurally related, particularly in the amino-terminal region, which confers DNA binding specificity, and they independently bind to a promoter element shared by the *IFN-α* and *IFN-β* genes as well as many IFN-inducible genes. This promoter element has the consensus sequence motif G(A)AAA(G or C)(T or C)GAAA(G or C)(T or C) (*5, 6*). IRF-1 and IRF-2 are distantly related in structure to two other DNA binding factors involved in IFN signaling, ICSBP and ISGF3γ (*3*).

Gene transfection studies have demonstrated that IRF-1 functions as an activator for IFN and IFN-inducible genes, whereas IRF-2 represses the action of IRF-1 (*5, 7–10*). Expression of the *IRF-1* gene itself is IFN-inducible. The *IRF-2* gene is also induced in IFN-stimulated cells, but this induction occurs only after induction of *IRF-1* (*5*). In IFN-treated or virus-infected cells, the IRF-2 protein is more stable than the IRF-1 protein (half-lives of 8 hours and 30 min, respectively) (*11*). Thus, in growing cells IRF-2 is more abundant than IRF-1, but after stimulation by IFN or viruses the amount of IRF-1 increases relative to IRF-2 (*11*). These observations suggest that a transient decrease in the IRF-2:IRF-1 ratio may be a critical event in the regulation of cell growth by IFNs. Consistent with this notion are the findings that IRF-1 manifests antiproliferative properties both in vivo and in vitro (*4, 12*).

We first quantified expression of *IRF-1* and *IRF-2* mRNAs in mouse NIH 3T3 cells throughout the cell cycle. Cells were growth-arrested by serum starvation for 24 hours (G_1 arrest) and were then induced to transit the cell cycle by serum restoration (*13*). A [^{3}H]thymidine uptake assay and

Institute for Molecular and Cellular Biology, Osaka University, Yamadaoka 1-3, Suita-shi, Osaka 565, Japan.

*The first two authors, to whom correspondence should be addressed, contributed equally to this work.

flow cytometric analysis revealed that DNA synthesis began 8 to 12 hours after serum stimulation (*14*). S1 analysis (*15*) indicated that *IRF-1* mRNA expression reached a peak (about five transcripts per cell) in growth-arrested cells, declined sharply after serum stimulation, and then increased gradually prior to the onset of DNA synthesis (Fig. 1A). In cells sampled 2 hours after stimulation, *IRF-1* mRNA expression was five times lower than in growth-arrested cells. In contrast, *IRF-2* mRNA expression remained essentially constant throughout the cell cycle. Protein immunoblotting analysis with antibodies to IRF-1 indicated that expression of the protein also oscillated throughout the cell cycle (*16*); IRF-1 expression peaked in the growth-arrested stage, declined, by a factor of 6, 3 hours after serum restoration, and subsequently increased again (Fig. 1B). Similar observations were made in an interleukin-3–dependent hematopoietic cell line, BAF-B03 (*17*), suggesting that this oscillation is not unique to NIH 3T3 cells.

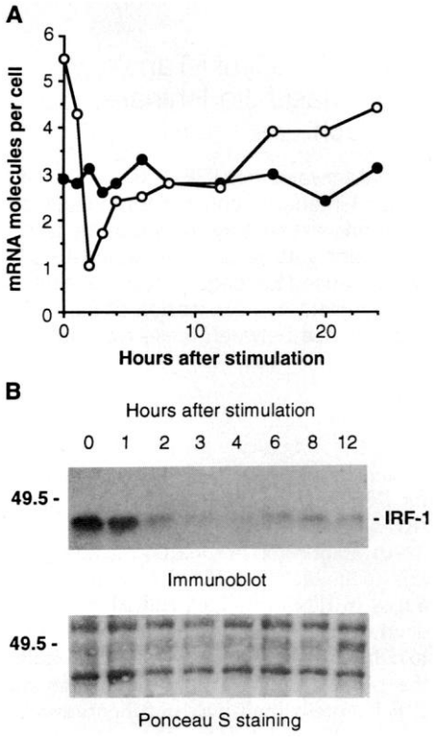

Fig. 1. Oscillation of *IRF-1* and *IRF-2* expression throughout the cell cycle. (**A**) Expression of *IRF-1* (open circles) and *IRF-2* (closed circles) mRNAs during serum-induced growth. NIH 3T3 cells were arrested by serum starvation and subsequently stimulated by serum addition. At the indicated times, total RNA was isolated and subjected to S1 analysis (*15*). Experiments were repeated three times and the results were reproducible. (**B**) Expression of IRF-1 protein during serum-induced growth. NIH 3T3 cells were growth-arrested and stimulated as in (A). Immunoblotting analysis was performed with whole cell extracts from 5×10^5 cells prepared at the indicated times. The filter was also stained with Ponceau S to show total protein (*16*). Molecular size in kilodaltons is indicated on the left. Experiments were repeated twice and the results were reproducible.

To examine the effect of perturbing the IRF-2:IRF-1 ratio on cell growth, we generated NIH 3T3 cell clones that overexpressed IRF-2. The plasmid pAct-2 (*9*), which contains mouse *IRF-2* cDNA cloned downstream of the chicken β-actin gene promoter, was cotransfected with a neomycin (*neo*)-resistance gene into NIH 3T3 cells (*18*). Control transfections were done with pAct-C, a plasmid devoid of the cDNA insert. After selection for *neo* resistance, we obtained several clones that expressed high levels of *IRF-2* mRNA and chose three (R21, R25, and R27) for further analysis. The expression of *IRF-2* mRNA in these cells was more than ten times higher than the basal expression observed in the pAct-C–transfected cells (C2 and C3) (Fig. 2) (*18*). The IRF-2 binding activities, monitored by gel-shift analysis (*9*), was four to ten times higher than in the control cells (Table 1) (*19*).

Although cells overexpressing IRF-2 did not exhibit obvious morphological changes, they displayed marked differences in growth properties. The IRF-2–overexpressing cells grew at a rate similar to that of control cells but reached a cell density that was about three times higher (Table 1). Furthermore, all of the IRF-2–overexpressing cells displayed anchorage-independent growth; they formed colonies in methylcellulose gel with an efficiency ranging from 6 to 19%, whereas no colony formation was seen with the control cells (Table 1). These properties often correlate with malignant transformation (*20*).

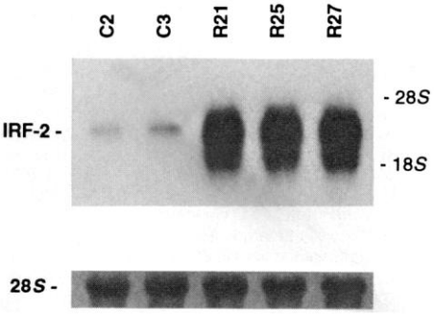

Fig. 2. Overexpression of *IRF-2* mRNA in NIH 3T3 cells. Five micrograms of RNA were subjected to RNA blot analysis. The filter was stained by methylene blue to show total RNA and then probed with a mouse *IRF-2* cDNA (*9*). The positions of 28*S* and 18*S* ribosomal RNAs are indicated.

When cells (2×10^6) from the R21, R25, and R27 clones were injected subcutaneously into nude mice, tumors developed within 2 to 3 weeks (Table 1) and continued to grow unrestrictedly, although they showed no signs of metastasis (*14*). No tumors developed in nude mice injected with cells from the control C2 and C3 clones during the same time period. Cells from an additional nine clones overexpressing *IRF-2* mRNA were also found to be tumorigenic in this assay (*14*). The cells recovered from the tumors exhibited essentially the same levels of *IRF-2* mRNA expression and growth properties as the original clones (*14*). These results indicate that the acquisition of altered growth properties and tumorigenicity was due to the elevated expression of IRF-2.

As another test of the oncogenic poten-

Table 1. Growth properties of control NIH 3T3 cells and NIH 3T3 cells overexpressing mouse *IRF-2*.

Cells	IRF-2:IRF-1 activity ratio*	Growth in monolayers†		Growth efficiency (%) in methylcellulose gel‡	Tumorigenicity§	
		Doubling time (hours)	Saturation density (10^6 cells)		Tumors per injection	Latency (weeks)
C2	10	30.6 ± 0.0	1.87 ± 0.06	0, 0	0/7	
C3	10	28.7 ± 0.8	1.87 ± 0.05	0, 0	0/5	
R21	101	25.7 ± 1.1	4.93 ± 0.14	7, 12	6/6	2 to 3
R25	42	28.8 ± 0.3	4.30 ± 0.04	6, 6	6/6	2 to 3
R27	78	27.5 ± 0.6	4.40 ± 0.01	10, 19	6/6	2 to 3

*The ratio of DNA binding activity was estimated by densitometric scans of autoradiograms from gel-shift analyses. †Cells were seeded at 2×10^4 cells per 35-mm plate and grown in DMEM supplemented with 10% FCS and G418 (700 μg/ml). Medium was changed every 3 days and cells were counted with a Coulter counter every 2 days. Doubling time was determined by calculating the growth rate of exponentially growing cells. Saturation density is the number of cells after the culture had reached confluency. The size of the cells in the selected clones was essentially the same as that of the parental cells. Numbers are the means of duplicate assays ± SD. ‡Cells (10^5) were mixed with 1.3% methylcellulose gel dissolved in culture medium and layered onto an agarose bed composed of 0.53% agarose and culture medium (*31*). Colonies were scored 3 weeks after plating. Each experiment was done in duplicate. A total of about 100 cells were counted for each assay ($P < 0.001$ by χ^2 test). §Four- to six-week-old nude mice (BALB/c nu/nu; Clea Japan, Inc.) were injected subcutaneously on both flanks with 2×10^6 cells resuspended in serum-free DMEM (200 μl) (*32*). Cells were scored as tumorigenic if a visible nodule appeared at the site of injection and subsequently increased in size. Mice that did not develop tumors were observed for 6 weeks.

Table 2. Efficiency of colony formation (percent) by NIH 3T3 and R27 cells after retroviral introduction of *IRF-2* or *IRF-1*.

Cells	Virus	Experiment number				
		1 (MOI = 10)	2 (MOI = 10)	3 (MOI = 0.3)	4 (MOI = 1)	5 (MOI = 10)
NIH 3T3*	pGD	<1, <1	<1, <1			
NIH 3T3*	pGDIRF2	17, 15	12, 16			
R27†	pGD			8.3, 7.8	8.4, 8.2	8.3, 8.6
R27†	pGDIRF1			6.1, 5.7	3.7, 4.5	3.9, 2.5

*NIH 3T3 cells were infected with recombinant retrovirus pGDIRF2 or control virus pGD (MOI = 10). After 48 hours, cells were harvested for the colony-forming assay in methylcellulose gel. Each experiment was done in duplicate. Stable integration of the proviral genome was virtually 100%, as determined by testing the *neo*-resistance of an aliquot of the cells. A total of 1000 cells were counted for each assay ($P < 0.001$ by χ^2 test). †R27 cells were infected at three different MOI with recombinant retrovirus pGDIRF1 or control virus pGD. Each experiment was done in duplicate. The colony-forming efficiency of the parental R27 cells was similar to that of the pGD-infected cells. A total of 5000 cells were counted for each assay ($P < 0.001$ by χ^2 test).

tial of IRF-2, we constructed a recombinant retrovirus vector, pGDIRF2, that directed expression of the mouse *IRF-2* cDNA (*21*). NIH 3T3 cells were infected with the pGDIRF2 retrovirus at a high multiplicity of infection (MOI) and the cells were directly tested in a colony-formation assay on methylcellulose gel. The cells infected by the IRF-2–expressing virus, but not by the control pGD virus, formed colonies at high efficiency (Table 2). Assuming that all the cells were infected by the virus, the colony-forming efficiency was similar to that of the R21, R25, and R27 clones (see Table 1). These results thus confirmed the oncogenic potential of IRF-2.

We next addressed whether the transformed phenotype displayed by NIH 3T3 cells overexpressing *IRF-2* could be reverted to the original phenotype by increasing the expression of *IRF-1*. To test this possibility, we introduced into the *IRF-2*–transfected cells a 19-kb DNA segment containing all ten exons, as well as the promoter region [455 bp upstream of the major cap site, (*22*)], of the human *IRF-1* gene. The R21, R25, and R27 cells were cotransfected with a plasmid (pUCHIRF1B) carrying the *IRF-1* gene and a hygromycin (*hgr*) resistance gene (*23*). Clones showing *hgr* resistance were selected and subsequently screened for stable integration of *IRF-1*.

The transfectants R21-1, R21-2, R25-2, R27-3, and R27-4 were derived from parental clones R21, R25, and R27. S1 analysis revealed steady-state expression of human *IRF-1* mRNA in most of these transfectants, albeit at different levels in each (Table 3). The transfected *IRF-1* gene was also virus-inducible in all clones (Table 3), and, in a separate set of experiments, it was shown that the promoter sequence within the cloned gene was also IFN-inducible (*22*). Expression of IRF-2 mRNA and protein, assessed by Northern (RNA) blotting and immunoprecipitation analyses, respectively, was similar to that in the parental cells (*14*). Interestingly, however, the tumorigenicity of the transfected cells was suppressed (Table 3). Moreover, the extent of suppression correlated with the extent of ectopic *IRF-1* mRNA expression. Clones R25-2 and R27-3, both of which expressed high amounts of human *IRF-1* mRNA, showed strong suppression; clones R27-4 and R21-1, which expressed lower amounts of *IRF-1* mRNA, showed somewhat weaker suppression; and clone R21-2, in which steady-state expression of human *IRF-1* mRNA was not detectable, showed no suppression (Table 3).

Concomitant with the loss or reduction of the transformed phenotype, the R21-1, R25-2, R27-3, and R27-4 cell clones exhibited a loss or reduction of other transformation-associated traits, such as increased cell saturation density and anchorage-independent growth (Table 3). Thus, the *IRF-2*–induced transformation of NIH 3T3 cells appears to be reversible by the introduction and increased expression of *IRF-1* (*24*). Consistent with this notion, there was a marked reduction in the colony-forming potential of R27 cells infected with a retrovirus (pGDIRF1) that directs the expression of mouse *IRF-1* (Table 2) (*21*).

The work presented here shows that transcription factors participating in the regulation of IFN-mediated effects also participate in cell growth regulation. We infer that the ability of IFNs to inhibit cell proliferation may be due, at least in part, to a transient induction of *IRF-1* (*5*); however, this possibility has not yet been directly tested. Presumably, overexpression of *IRF-2* induces cell transformation by suppressing the cell growth–restraining function of IRF-1. Although the mechanism by which IRF-1 and IRF-2 affect cell growth is unknown, we think it is likely that IRF-1 functions in a manner analogous to the tumor suppressor p53 (*25*), that is, it activates a set of genes whose products are required for the negative regulation of cell growth. IRF-2, on the other hand, may repress those same genes. This ying-yang interaction may be similar to that of another tumor suppressor, WT1, and its antagonist EGR-1, which function as a repressor and an activator, respectively (*26*). Many, if not all, of the IFN-inducible genes contain promoter elements that bind IRFs (*1, 9, 10*), and some of their gene products, such as the 2′-5′ oligoadenylate synthetase and double-stranded RNA-dependent protein kinase (dsRNA-PK), appear to be involved in the inhibition of cell proliferation (*1, 27*). Interestingly, the activity of the 2′-5′ oligoadenylate synthetase seems to oscillate throughout the cell cycle (*28*), and its expression is regulated by IRF-1 (*8*). The dsRNA-PK itself has recently been shown to have anti-oncogenic potential (*29*).

Finally, the anti-oncogenic function of the *IRF-1* gene is supported by its chromosomal location. The human *IRF-1* gene maps to chromosome 5q31.1, a region frequently deleted in patients with leukemia or myelodysplastic syndromes (*30*).

Table 3. Growth properties of NIH 3T3 cells overexpressing mouse *IRF-2* and human *IRF-1*.

Cells	Human *IRF-1* mRNA expression (transcripts per cell)*		Growth in monolayers		Growth efficiency (%) in methylcellulose gel	Tumorigenicity	
	Steady state	NDV induced	Doubling time (hours)	Saturation density (10^6 cells)		Tumors per injection	Latency (weeks)
R21-1	1	6	28.0 ± 0.1	2.66 ± 0.11	4, 4	2/6	2
R21-2	ND	7	28.1 ± 0.2	3.72 ± 0.38	6, 8	6/6	2 to 3
R25-2	24	463	28.9 ± 0.3	2.04 ± 0.37	0, 0	0/5	
R27-3	16	542	28.8 ± 1.5	1.67 ± 0.07	0, 1	0/6	
R27-4	3	65	29.8 ± 1.1	2.52 ± 0.02	5, 5	3/6	3 to 3.5

*Each clone was mock-induced or induced by Newcastle disease virus (NDV) as described previously (*2*). After 9 hours, total RNA was isolated and subjected to S1 analysis (*9*). The *IRF-1* probe DNA encompasses nucleotides −46 to +97 (relative to the major cap site at +1) of the human *IRF-1* gene. All other assays were performed as described in Table 1. For comparison, the growth properties of the parental clones R21, R25, and R27 are presented in Table 1. ND, not detectable.

REFERENCES AND NOTES

E. De Maeyer and J. De Maeyer-Guignard, *Interferons and Other Regulatory Cytokines* (Wiley, New York, 1988); J. Vilček, in *Peptide Growth Factors and Their Receptors: Handbook of Experimental Phar-*

macology, M. A. Sporn and A. B. Roberts, Eds. (Springer-Verlag, Berlin, 1990), pp. 3–38; I. Gresser, *Acta Oncol.* **28**, 347 (1989); N. Tanaka and T. Taniguchi, *Adv. Immunol.* **52**, 263 (1992).
2. T. Fujita *et al.*, *EMBO J.* **7**, 3397 (1988).
3. M. Miyamoto *et al.*, *Cell* **54**, 903 (1988); R. Pine, T. Decker, D. S. Kessler, D. E. Levy, J. E. Darnell, Jr., *Mol. Cell. Biol.* **10**, 2448 (1990); L.-Y. Yu-Lee, J. A. Hrachovy, A. M. Stevens, L. A. Schwarz, *ibid.*, p. 3087; P. H. Driggers *et al.*, *Proc. Natl. Acad. Sci. U.S.A.* **87**, 3743 (1990); S. A. Veals *et al.*, *Mol. Cell. Biol.* **12**, 3315 (1992).
4. A. Abdollahi, K. A. Lord, B. Hoffman-Liebermann, D. Liebermann, *Cell Growth Differ.* **2**, 401 (1991).
5. H. Harada *et al.*, *Cell* **58**, 729 (1989); T. Taniguchi, T. Fujita, H. Harada, J. Sakakibara, N. Watanabe, in *Origins of Human Cancer*, J. Brugge, T. Curran, E. Harlow, F. McCormick, Eds. (Cold Spring Harbor Laboratory, Cold Spring Harbor, NY, 1991), pp. 501–512.
6. This consensus sequence was determined by a random oligonucleotide selection method (N. Tanaka, unpublished data).
7. T. Fujita, Y. Kimura, M. Miyamoto, E. L. Barsoumian, T. Taniguchi, *Nature* **337**, 270 (1989); D. Näf, S. E. Hardin, C. Weissmann, *Proc. Natl. Acad. Sci. U.S.A.* **88**, 1369 (1991).
8. W.-C. Au, N. B. K. Raj, R. Pine, P. M. Pitha, *Nucleic Acids Res.* **20**, 2877 (1992); L. F. L. Reis, H. Harada, J. D. Wolchok, T. Taniguchi, J. Vilček, *EMBO J.* **11**, 185 (1992).
9. H. Harada *et al.*, *Cell* **63**, 303 (1990).
10. G. R. Stark and I. M. Kerr, *J. Interferon Res.* **12**, 147 (1992).
11. N. Watanabe, J. Sakakibara, A. G. Hovanessian, T. Taniguchi, T. Fujita, *Nucleic Acids Res.* **19**, 4421 (1991); N. Watanabe and T. Taniguchi, unpublished data.
12. G. Yamada *et al.*, *Proc. Natl. Acad. Sci. U.S.A.* **88**, 532 (1991); S. Kirchhoff *et al.*, *J. Interferon Res.* **12**, S102 (1992); N. Tanaka and T. Taniguchi, unpublished data.
13. NIH 3T3 cells were maintained in Dulbecco's modified Eagle's medium (DMEM) containing 10% fetal calf serum (FCS). For analysis of IRF-1 expression throughout the cell cycle, cells were grown to confluency and placed in serum-free DMEM for 24 hours, then stimulated by the addition of DMEM supplemented with 10% FCS, and harvested at the indicated times.
14. H. Harada, M. Kitagawa, H. Yamamoto, K. Harada, T. Taniguchi, unpublished data.
15. Total cellular RNA was isolated by the guanidinium-thiocyanate method. S1 analysis was performed as described previously [T. Fujita *et al.*, *Cell* **49**, 357 (1987)]. The mouse *IRF* probes were the same as described in (*9*).
16. Cell extracts were prepared by a slight modification of the method described in N. Dyson, L. A. Duffy, and E. Harlow [in *Molecular Diagnostics of Human Cancer*, M. Furth and M. Greaves, Eds. (Cold Spring Harbor Laboratory, Cold Spring Harbor, NY, 1989), pp. 235–240] and subjected to 12.5% SDS–polyacrylamide gel electrophoresis. The separated proteins were electrophoretically transferred to a polyvinylidene difluoride membrane filter and then stained with Ponceau S nonspecific dye [E. Harlow and D. Lane, *Antibodies* (Cold Spring Harbor Laboratory, Cold Spring Harbor, NY, 1988)]. Immunodetection was carried out as described previously [M. Hatakeyama *et al.*, *Science* **252**, 1523 (1991)] with a mixture of monoclonal antibodies to mouse IRF-1 (TK-1 and TK-3, 10 μg/ml each) (T. Kimura and T. Taniguchi, unpublished data).
17. M. Yoneyama and T. Taniguchi, unpublished data.
18. Fifteen micrograms of plasmid pAct-2 (*9*) were cotransfected with 0.3 μg of plasmid pSTneoB, which carries a *neo*-resistance gene [K. Katoh, Y. Takahashi, S. Hayashi, H. Kondoh, *Cell Struc. Funct.* **12**, 575 (1987)], into NIH 3T3 cells (5×10^5 cells per 10-cm dish) by the calcium phosphate method [T. Fujita *et al.*, *Cell* **41**, 489 (1985)]. The transfected cells were then selected in medium containing G418 (700 μg/ml), and resistant colonies were isolated after 2 to 3 weeks. Control cell lines (C2 and C3) were derived from cells transfected with the parental vector, pAct-C (*9*).
19. The IRF-1 binding activities were not increased in these clones.
20. V. H. Freedman and S. Shin, *Cell* **3**, 355 (1974); E. J. Keath, P. G. Caimi, M. D. Cole, *ibid.* **39**, 339 (1984).
21. Recombinant retroviruses pGDIRF1 and pGDIRF2 were constructed by inserting the mouse *IRF-1* or *IRF-2* cDNA into the pGD vector [G. Q. Daley, R. A. Van Etten, D. Baltimore, *Science* **247**, 824 (1990)]. The DNA constructs were transfected into ψ2 cells [R. Mann, R. C. Mulligan, D. Baltimore, *Cell* **33**, 153 (1983)], which subsequently released into the culture medium a high titer ($\sim 10^6$ colony-forming units per milliliter) of virus, as assayed by the ability to confer *neo* resistance to NIH 3T3 cells. Expression of the IRF-1 or IRF-2 protein in NIH 3T3 cells infected with the recombinant retroviruses was confirmed by gel-shift analysis.
22. S. Itoh, thesis, Osaka University (1990); K. Harada and H. Harada, unpublished data.
23. To obtain cell clones that expressed elevated amounts of IRF-1, we cotransfected 15 μg of plasmid pUCHIRF1B, a derivative of pUC19 carrying the 19-kb human *IRF-1* gene (*21*) at the Eco RI site (S. Itoh and T. Taniguchi, unpublished data), with 0.3 μg of plasmid pMiwhgh, which carried the *hgr* resistance gene [K. Kato, A. Kanamori, H. Kondoh, *Mol. Cell. Biol.* **10**, 486 (1990)] into R21, R25, or R27 cells (5×10^5 cells per 10-cm dish) by the calcium phosphate method. Cells were selected in medium containing hygromycin (100 μg/ml), and the *hgr*-resistant colonies isolated after 2 to 3 weeks.
24. The reduction in tumorigenicity of clones R27-3 and R27-4 was accompanied by a reduction in their IRF-2:IRF-1 activity ratio to a value similar to that of the C2 and C3 controls.
25. A. J. Levine, J. Momand, C. A. Finlay, *Nature* **351**, 453 (1991); B. Vogelstein and K. W. Kinzler, *Cell* **70**, 523 (1992).
26. S. L. Madden *et al.*, *Science* **253**, 1550 (1991); D. A. Haber and D. E. Housman, *Adv. Cancer Res.* **59**, 41 (1992); V. van Heyningen and N. D. Hastie, *Trends Genet.* **8**, 16 (1992).
27. M. Revel and J. Chebath, *Trends Biochem. Sci.* **11**, 166 (1986).
28. H. Jacobsen, D. Krause, R. M. Friedman, R. H. Silverman, *Proc. Natl. Acad. Sci. U.S.A.* **80**, 4954 (1983); V. Wells and L. Mallucci, *Exp. Cell Res.* **159**, 27 (1985).
29. A. E. Koromilas, S. Roy, G. N. Barber, M. G. Katze, N. Sonenberg, *Science* **257**, 1685 (1992); E. F. Meurs *et al.*, *Proc. Natl. Acad. Sci. U.S.A.*, in press.
30. S. Itoh, H. Harada, Y. Nakamura, R. White, T. Taniguchi, *Genomics* **10**, 1097 (1991); C. L. Willman *et al.*, *Science* **259**, 968 (1993); T. Hori and H. Harada, unpublished data.
31. K. Miyashita and T. Kakunaga, *Cell* **5**, 131 (1975).
32. S. Shin, *Methods Enzymol.* **58**, 370 (1979).
33. We thank H. Kondoh and M. L. Scott for the pMiwhgh and pGD vectors, respectively; E. Barsoumian, M. Lamphier, and C. Willman for advice and critical reading of the manuscript; and M. Yoneyama for help with the cell cycle analysis. This work was supported in part by a grant-in-aid for Special Project Research, Cancer Bioscience, from the Ministry of Education, Science, and Culture of Japan; by research grants from the Princess Takamatsu Cancer Research Fund and Takeda Science Foundation (to T.T.); and by a grant from Kato Memorial Bioscience Foundation (to H.H.). M.K. is supported by fellowships of the Japan Society for the Promotion of Science for Japanese Junior Scientists.

15 October 1992; accepted 11 December 1992

"Infectious" Transplantation Tolerance

Shixin Qin, Stephen P. Cobbold, Heather Pope, James Elliott, Dimitris Kioussis, Joanna Davies, Herman Waldmann*

The maintenance of transplantation tolerance induced in adult mice after short-term treatment with nonlytic monoclonal antibodies to CD4 and CD8 was investigated. $CD4^+$ T cells from tolerant mice disabled naïve lymphocytes so that they too could not reject the graft. The naïve lymphocytes that had been so disabled also became tolerant and, in turn, developed the capacity to specifically disable other naïve lymphocytes. This process of "infectious" tolerance explains why no further immunosuppression was needed to maintain long-term transplantation tolerance.

A major goal of transplantation is that the recipient should accept and become tolerant to a foreign organ graft as though it were a "self" tissue. The classic experiments of Medawar and colleagues (*1*) established this principle in the neonatal mouse. In the adult mouse lifelong tolerance can also be achieved with short courses of monoclonal antibodies (MAbs) to CD4 plus CD8 (*2–4*) or CD11a plus intercellular adhesion molecule-1 (ICAM-1) (*5*), even though new T cells continue to be made by the thymus. We wished to determine the mechanisms that might operate to keep the proliferation of such new T cells in check. A clue was provided by the finding that we could not break tolerance by transfusions of normal naïve lymphocytes (*3*). Consequently, we reasoned that if we could establish the mechanism by which these naïve lymphocytes become disabled, we might understand the processes controlling any new T cells produced by the body.

In order to follow events in a stable peripheral T cell pool, we used mice that had been thymectomized (ATx) at 4 to 6 weeks of age. Such ATx CBA/Ca mice

S. Qin, S. P. Cobbold, H. Pope, J. Davies, H. Waldmann, Department of Pathology, University of Cambridge, Cambridge CB2 1QP, United Kingdom.
J. Elliott and D. Kioussis, Laboratory of Molecular Immunology, National Institute for Medical Research, Mill Hill, London NW7 1AA, United Kingdom.

*To whom correspondence should be addressed.